Geophysical Research Letters®

Key Points:

- CAM6-Oslo and CAM6 capture the vertical structure of Arctic mixed-phase clouds, with supercooled liquid cloud tops overlying icy interiors
- Removing an invalid limit on heterogeneous and secondary ice nucleation processes in CAM6 reduces supercooled liquid water in Arctic clouds
- Parametrizations of mixed-phase processes control longwave cloud feedback by modifying how winter and spring clouds respond to warming

Correspondence to:

J. Shaw,
jonah.shaw@colorado.edu

Using Satellite Observations to Evaluate Model Microphysical Representation of Arctic Mixed-Phase Clouds

J. Shaw[1,2] [ID], **Z. McGraw[1,3]** [ID], **O. Bruno[4]** [ID], **T. Storelvmo[1,5]** [ID], **and S. Hofer[1]** [ID]

[1]Department of Geosciences, University of Oslo, Oslo, Norway, [2]Now at Department of Atmospheric and Oceanic Sciences, University of Colorado at Boulder, Boulder, CO, USA, [3]Now at Department of Applied Physics and Applied Mathematics, Columbia University and NASA Goddard Institute for Space Studies, New York, NY, USA, [4]Karlsruhe Institute of Technology, Institute of Meteorology and Climate Research, Karlsruhe, Germany, [5]School of Business, Nord University, Bodø, Norway

Abstract Mixed-phase clouds play an important role in determining Arctic warming, but are parametrized in models and difficult to constrain with observations. We use two satellite-derived cloud phase metrics to investigate the vertical structure of Arctic clouds in two global climate models that use the Community Atmosphere Model version 6 (CAM6) atmospheric component. We report a model error limiting ice nucleation, produce a set of Arctic-constrained model runs by adjusting model microphysical variables to match the cloud phase metrics, and evaluate cloud feedbacks for all simulations. Models in this small ensemble uniformly overestimate total cloud fraction in the summer, but have variable representation of cloud fraction and phase in the winter and spring. By relating modeled cloud phase metrics and changes in low-level liquid cloud amount under warming to longwave cloud feedback, we show that mixed-phase processes mediate the Arctic climate by modifying how wintertime and springtime clouds respond to warming.

Plain Language Summary Clouds are important regulators of warming in the Arctic. The thermodynamic phase of a cloud affects its lifetime and transparency to incoming and outgoing radiation. As a result, transitions from ice to liquid in a warming climate change the influence of clouds on surface temperature. At temperatures between −37°C and 0°C, both ice and supercooled liquid water may exist simultaneously in a cloud layer. Global climate models struggle to capture cloud phase in this temperature range because it depends on both cloud temperature and aerosol properties. This study investigates how the fraction of supercooled liquid water changes vertically in Arctic clouds, comparing liquid-rich cloud tops with their icy interiors. We describe a significant model error that limits the formation of new ice crystals. We also find that global climate models reproduce observations, and that a range of model parameters produce results consistent with observations. Changes in cloud fraction resulting from these adjustments mostly occur in the winter and spring, and cause the models to trap longwave radiation differently. The results of this study highlight the need to capture seasonal changes in cloud phase and amount in order to successfully predict future changes to the Arctic climate.

1. Introduction

Uncertainties in cloud and aerosol radiative effects are a principal contributor to climate model uncertainty, and remain so despite decades of model development (Boucher et al., 2013). These uncertainties arise from the difficulty of representing aerosol–cloud interactions and other key physical processes at the typical resolutions of global climate models (GCMs). Evaluations of available models from the Coupled Model Intercomparison Project Phase 6 (CMIP6; Eyring et al., 2016) indicate that changes in climate sensitivity relative to CMIP5 (Taylor et al., 2012) are mostly due to changes in cloud representation, specifically for extratropical low-level clouds (Zelinka et al., 2020). Using observations to reevaluate the representation of these clouds in the latest generation of GCMs is a vital part of testing the validity of these new predictions.

In the Arctic, clouds mediate climate change through interactions with land and sea ice, and impacts on surface radiative fluxes (H. Morrison et al., 2012). As the thermodynamic phase of Arctic clouds shifts from ice to liquid in response to warming, the radiative effect they exert on the surface changes (Mitchell et al., 1989). This cloud phase feedback depends on cloud optical thickness and lifetime changes. In the Arctic, observations indicate that liquid and ice clouds exert very different radiative forcings on the surface (Cesana et al., 2012; Shupe &

Writing – original draft: J. Shaw
Writing – review & editing: J. Shaw, T. Storelvmo, S. Hofer

Intrieri, 2004), highlighting the need for models to capture cloud phase in order to produce a realistic surface energy budget.

At temperatures between approximately −37°C and 0°C, cloud ice forms via heterogeneous nucleation processes that are dependent on temperature, in-cloud vapor pressure, and the presence of ice nucleating particles (INPs; Korolev, 2007). Cloud ice and water can coexist as mixed-phase clouds in this regime. The fraction of super-cooled liquid water in a mixed-phase cloud layer can be referred to as the supercooled liquid fraction (SLF; Komurcu et al., 2014). Observations show that Arctic mixed-phase clouds are both common and long-lived (Matus & L'Ecuyer, 2017; H. Morrison et al., 2012), due in part to their vertical structure in which INP-limited liquid cloud tops are separated from glaciated interiors, preventing ice from quickly depleting cloud water and allowing clouds to persist for several days (Hobbs & Rangno, 1998). Through this effect on cloud lifetime and opacity, cloud top phase mediates the resulting long- and shortwave cloud feedbacks.

Model representation of mixed-phase clouds relies on uncertain parameters. Several studies of mixed-phase clouds in the Community Atmosphere Model Version 5 (CAM5) have found that the Wegener–Bergeron–Findeisen (WBF) process time scale has the largest role in determining liquid cloud fraction (Huang et al., 2021; McIlhattan et al., 2017; Tan & Storelvmo, 2016), with Huang et al. (2021) finding that reducing the WBF time scale was primarily important in INP-limited environments. High-resolution modeling studies of Arctic mixed-phase clouds also indicate that cloud phase is highly sensitive to ice formation mechanisms and the availability of INPs (Fridlind et al., 2007; Fu et al., 2019; Jiang et al., 2000). Because INP concentrations and the strength of the WBF process specifically impact mixed-phase clouds and have large reasonable ranges, they make appropriate tuning parameters for GCM experiments (Mauritsen et al., 2012).

Observations of cloud fraction and phase obtained from the Cloud-Aerosol Lidar with Orthogonal Polarization (CALIOP) sensor aboard the CALIPSO platform provide a strong observational constraint for assessing cloud representation in GCMs (Winker et al., 2009). Cloud phase is especially important, as observations of cloud fraction alone may hide compensating phase biases with large radiative impacts (Cesana & Chepfer, 2012). Using CALIOP cloud phase products, Cesana et al. (2012) found that radiatively clear (opaque) atmospheric states in the Arctic were characterized by the absence (presence) of liquid cloud. This result supported the findings of Shupe and Intrieri (2004) and demonstrated that satellite retrievals of cloud phase can be effectively used to study the Arctic surface energy budget.

Comparing CAM6 to cloud phase observations is enabled by the use of definition- and scale-aware cloud phase variables produced by the Cloud Feedback Model Intercomparison Project (CFMIP) Observational Simulator Package: Version 2 (COSP2; Swales et al., 2018). With new heterogeneous ice nucleation (Hoose et al., 2008) and stratiform cloud microphysics (H. Morrison & Gettelman, 2008) schemes in CAM6 causing significant changes to precipitation and cloud fraction over the Greenland Ice Sheet (Lenaerts et al., 2020), further investigation of cloud representation over the entire Arctic region is well motivated.

Recent studies of Arctic feedbacks highlight the importance of the temperature and albedo feedbacks (Pithan & Mauritsen, 2014), noting the lack of a cloud response to summer sea ice loss (A. L. Morrison et al., 2018). While longwave cloud feedbacks are believed to play a secondary role in Arctic warming, large uncertainties associated with mixed-phase processes have yet to be evaluated.

In the Arctic, both CMIP5 models and reanalysis data products struggle to reproduce observed cloud phase and optical depth (Lenaerts et al., 2017). Because many Arctic feedbacks are non-linear, this inability to capture the mean state influences projected cloud feedbacks (Goosse et al., 2018). Targeted modeling experiments which capture the observed mean state are valuable tools for disentangling the roles of different Arctic feedback mechanisms and evaluating model parameterizations (Kay et al., 2016). Tan and Storelvmo (2019) found that minimizing global cloud phase biases in the CESM1 model yielded a broad range of cloud microphysical variables and Arctic Amplification factors. This study, however, did not examine whether the global model adjustments created a reasonable representation of cloud phase in the Arctic itself or distinguish between remote and local drivers of Arctic feedbacks (Feldl et al., 2020). We address this concern by focusing our model adjustments and analysis on the Arctic and assessing model performance with additional observational constraints. Atmosphere-only simulations isolate how the microphysical representation of mixed-phase clouds impacts Arctic warming. Whereas the fully-coupled simulations of Tan and Storelvmo (2019) investigated the Arctic impact of a global SLF correction, this work specifically investigates how and why local cloud microphysics affect the Arctic.

2. Methods

2.1. Cloud Phase Metrics

To investigate the vertical structure of mixed-phase clouds, we filter by overlying cloud optical thickness (COT) to produce two SLF metrics. We obtain one metric (hereafter: cloud top SLF) by selecting only the highest layer of observed mixed-phase clouds after discarding the uppermost layers with COT <0.3 in order to avoid including optically thin cirrus clouds. Another metric (hereafter: cloud-bulk SLF) is obtained by selecting all cloud layers retrieved by CALIOP with overlying COT less than 3.0. Validation of the cloud bulk metric, as well as methodology for calculating the observational and modeled SLF metrics are described in the Supplementary Material. SLF is calculated on isotherms from $-40°C$ to $0°C$, with a $5°C$ increment. Measurements of cloud phase were retrieved from NASA's CALIOP instrument (Winker et al., 2009) for a 4 year observational period from June 1, 2009 through May 31, 2013.

2.2. Additional Satellite Products

To conduct further model evaluation of cloud fraction and radiative fluxes, we compare against the GCM–Oriented CALIPSO Cloud Product (GOCCP) Version 3 (Chepfer et al., 2010) and Clouds and the Earth's Radiant Energy System Energy Balanced and Filled (CERES-EBAF) Ed4.0 datasets (Kato et al., 2018). The GOCCP data product ($82°S–82°N$) separates total cloud fraction by phase, and is produced specifically for comparison with the COSP satellite simulator. From CERES-EBAF, we use computed surface long- and shortwave cloud radiative effect (CRE) values and surface all-sky downwelling fluxes.

2.3. Modeling Simulations

We present atmosphere-only runs of the Nordic Earth System Model Version 2 (NorESM2; Seland et al., 2020) and the Community Earth System Model Version 2 (CESM2; Danabasoglu et al., 2020). Both models have 32 vertical levels and are run at $1.9° \times 2.5°$ horizontal resolution. We use identical model components in both GCMs to isolate the impact of differences between the atmospheric modules. While both models use CAM6, CESM2 uses the MAM4 aerosol scheme (Liu et al., 2016), and NorESM2 uses the OsloAero5.3 (Kirkevåg et al., 2018) aerosol scheme while also parametrizing mid- and high-level ice clouds differently. Runs of NorESM2 and CESM2 are subsequently referred to as CAM6-Oslo and CAM6. All modeled data represent averages over the same 4-year period from which SLF values were calculated following a 3-month model windup to allow the atmosphere to adjust to microphysics changes. To reduce variability in meteorology between runs, we nudge horizontal winds and surface pressure to ERA-Interim reanalysis data for the observational period (Dee et al., 2011). Because sea ice concentrations are prescribed, these simulations do not explore cloud-sea ice feedbacks.

2.4. Model Modifications

INP availability is an important limiting factor in cloud glaciation at mixed-phase temperatures. In CAM6 and CAM6-Oslo, the in-cloud ice number concentration cannot exceed the calculated concentration of available ice nuclei. Neither heterogeneous nor secondary nucleation processes contribute to this INP limit, preventing them from nucleating ice crystals. Heterogeneous nucleation processes are still able to increase ice crystal mass, however, and can artificially inflate ice crystal size and increase sedimentation. This model error has been shared with model developers and identified as an issue to be resolved in future releases of CAM (personal communications, A. Gettelman, 2021), and one global correction significantly alters the climate sensitivity of CESM2 (Zhu et al., 2021).

To assess the importance of this model mechanism on cloud properties and ice number concentration and size, we disable the ice number limit at mixed-phase temperatures ($-37°C < T < 0°C$) in CAM6-Oslo, restoring heterogeneous ice production as well as secondary ice production through the Hallet–Mossop process, and producing an additional model variation we label as CAM6-OsloIce. To isolate the impact of heterogeneous nucleation, we also cap the ice number tendency variable from secondary ice production in CAM6-OsloIce to avoid strong secondary production in the absence of the ice number limit, describing this implementation in the Supporting Information. To focus on Arctic clouds, these changes are made only in the Arctic Circle (latitude $>66°N$). Whereas mixed-phase clouds in CAM6 are strongly (and potentially unrealistically) INP-limited by the ice number limit,

Table 1
Model Run Descriptions

Run name	Model	Ice number limit (secondary ice limit)	WBF multiplier	INP multiplier	Average ice radius at 860 hPa (μm)	Ice concentration at 860 hPa (m^{-3})
CAM6-Oslo	NorESM2	Yes (No)	1.0	1.0	151	4,120
CAM6	CESM2	Yes (No)	1.0	1.0	165	5,550
CAM6-OsloIce	NorESM2	No (Yes)	1.0	1.0	132	15,670
CAM6-Oslo Fit 1	NorESM2	Yes (No)	1.25	10.0	163	3,870
CAM6-OsloIce Fit 2	NorESM2	No (Yes)	0.5	0.05	124	5,410
CAM6-OsloIce Fit 3	NorESM2	No (Yes)	0.2	0.1	112	8,600
CAM6 Fit 4	CESM2	Yes (No)	1.0	100	209	5,060
CAM6-Olso(1.25,1)	NorESM2	Yes (No)	1.25	1.0	156	3,950
CAM6-Olso(1,10)	NorESM2	Yes (No)	1.0	10.0	160	4,020
CAM6-OsloIce(0.2,1)	NorESM2	No (Yes)	0.2	1.0	112	23,460
CAM6-OsloIce(0.5,1)	NorESM2	No (Yes)	0.5	1.0	123	16,540
CAM6-OsloIce(1,0.05)	NorESM2	No (Yes)	1.0	0.05	134	4,250
CAM6-OsloIce(1,0.1)	NorESM2	No (Yes)	1.0	0.1	134	4,430

Note. Prenni et al. (2009) reported an average INP concentration of 700 m^{-3} and a maximum INP concentration 6,000 m^{-3} from the M-PACE experiment

CAM6-OsloIce serves as an alternate ensemble end-member representing the assumption that transport and entrainment bring in fresh INPs to replace those that nucleated ice in the previous model time step.

Using nudged 12-month simulations, we iteratively modify the time scale of the WBF process and the number of aerosols active as INPs in the base models (CAM6-Oslo, CAM6, and CAM6-OsloIce) to minimize root-mean-square error with the SLF metrics. Methodology for parameter tuning ranges and validation of ice crystal concentrations is described in the Supporting Information. This approach produced four "fitted" models that agree with observations. Table 1 summarizes the three base models and four "fitted" models presented in this work, as well as six ancillary simulations in which single parameters were tuned to the "fitted" values. When the ice limit is in place, large INP multipliers increase ice crystal size and decrease the ice number concentration (CAM6 Fit 4 vs. CAM6, CAM6-Oslo vs. CAM6-Oslo(1,10)), demonstrating nonphysical behavior caused by the model error. Conversely, runs without an ice number limit have smaller ice crystals and higher concentrations than those with the limit in place. Ice crystal size and concentration variables in the constrained runs (Table 1) fall near observed ranges from the M-PACE experiment (Prenni et al., 2009), preventing us from discarding any of the simulations.

2.5. Radiative Feedback Calculations

We use surface radiative kernels from Soden et al. (2008) to calculate long- and shortwave cloud feedback parameters. We repeat each simulation from Table 1 with prescribed sea surface temperatures increased by 4K globally to create perturbed runs for the radiative feedback calculations. Because we run atmosphere-only simulations and modify models only poleward of 66°N, feedback parameters are calculated with respect to the temperature change in the Arctic rather than the global mean.

3. Results

3.1. SLF Metrics

Figure 1a shows the SLF metrics from CALIOP observations and the base models. In the CALIOP retrievals, cloud top SLF is greater than cloud-bulk SLF values for all isotherms between −35°C and −10°C. At −20°C where this difference is the most pronounced, cloud top SLF exceeds the cloud-bulk value by nearly a factor of three. All models reproduce the structure of icier cloud interiors, but with varying degrees of quantitative agreement with CALIOP: CAM6-Oslo shows strong agreement across both metrics, CAM6 overestimates SLF in cloud tops, and CAM6-OsloIce underestimates SLF along both the cloud top and cloud-bulk SLF metrics.
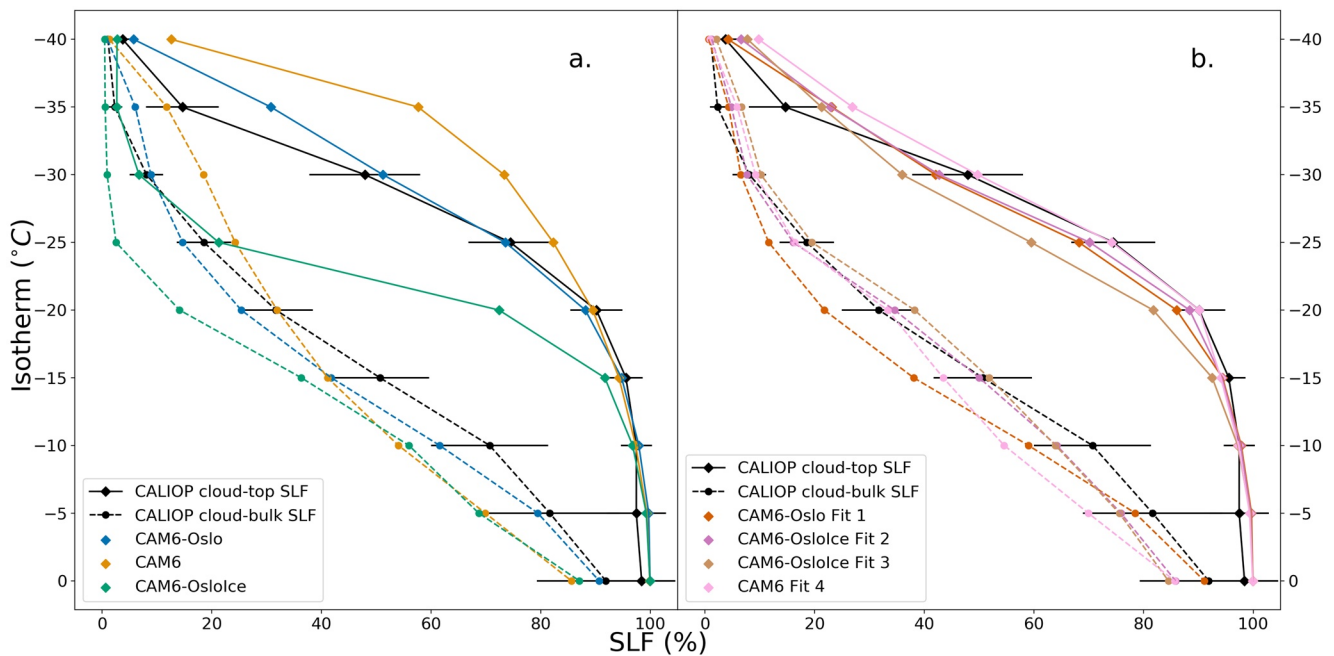
Figure 1. Supercooled liquid fraction by isotherm for cloud top and cloud-bulk metrics for (a) base models and (b) fitted models. Error bars on CALIOP SLF values correspond to one standard deviation. All values represent an area-weighted average from 66° to 82°N.

The poor performance of CAM6-OsloIce results from a high ice number concentration that allows liquid water to be quickly depleted. Differences in SLF between CAM6-Oslo and CAM6-OsloIce mostly occur at cold isotherms where secondary ice processes are not active, showing that freed heterogeneous nucleation processes are responsible for the cloud changes between these models and that environments with few INPs are necessary for maintaining liquid cloud tops below 20°C. Figure 1b shows SLF metrics for CALIOP and the fitted models.

3.2. Evaluation Against CALIOP-GOCCP and CERES-EBAF Data Products

Monthly averages of cloud fraction by CALIOP phase designation allow us to identify seasonal trends and biases (Figure 2). We find that fitting to the SLF metrics brings CAM6-Oslo and CAM6-OsloIce models into good agreement with each other, indicating that the effect of removing the limit on ice number can be compensated for with the adjustment of the WBF and INP parameters. In the summer and early fall, the total cloud fraction and the liquid and ice components are consistent across all models, with an overestimation of liquid and total cloud fraction during June and July. Differences between models emerge in the winter and spring months. CAM6-OsloIce, CAM6-Oslo Fit 1, CAM6-Oslo Fit 2, and CAM6 Fit 4 all produce insufficient total cloud fraction during the winter, while CAM6 produces excess total cloud fraction. All models fail to capture the total cloud fraction in the spring, mostly due to insufficient ice cloud fraction. Finally, a positive liquid cloud bias in CAM6 persists throughout the year and is especially pronounced during the winter.

Annual model biases in Arctic-averaged cloud fraction and CRE with respect to CALIOP-GOCCP and CERES-EBAF (Table S1 in Supporting Information S1) follow the results of Figure 2. Notable compensating biases in cloud fraction by phase are present, with CAM6 producing excess liquid cloud and insufficient ice cloud, and CAM6-OsloIce producing excess ice cloud and insufficient liquid cloud. CAM6 Fit 4 shares the ice cloud bias of CAM6 despite having good agreement with the observed SLF metrics because positive biases in mid- and high-level ice clouds are unaffected by the model adjustments. Polar projections of model cloud phase biases (Figure S2 in Supporting Information S1) show the spatial features of model cloud phase biases.

All simulations have negative shortwave CRE biases between -2.9 and -5.1 Wm^{-2} on the annual mean due to the shared positive cloud fraction bias in the summer. Downwelling shortwave surface flux and CRE biases (Figures 3a and 3b) strongly resemble each other, confirming that clouds are responsible for the shortwave biases. Excessive summer cloudiness is largely independent of mixed-phase processes, since low-level liquid clouds
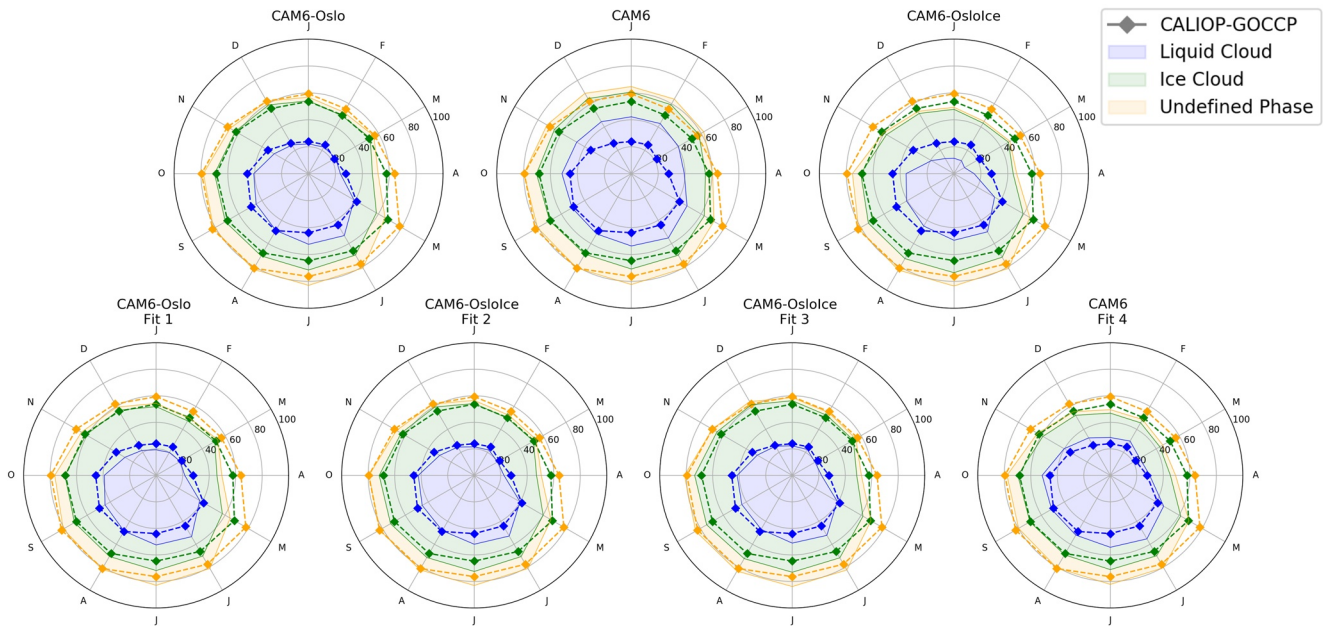
Figure 2. Comparison of monthly cloud fraction by phase. Model values are produced by the COSP CALIPSO satellite simulator and observations are from the CALIPSO-GOCCP cloud phase products. The different cloud phase components are stacked on top of each other so that the outermost contour gives the total cloud fraction and compensating phase biases can be easily visualized.
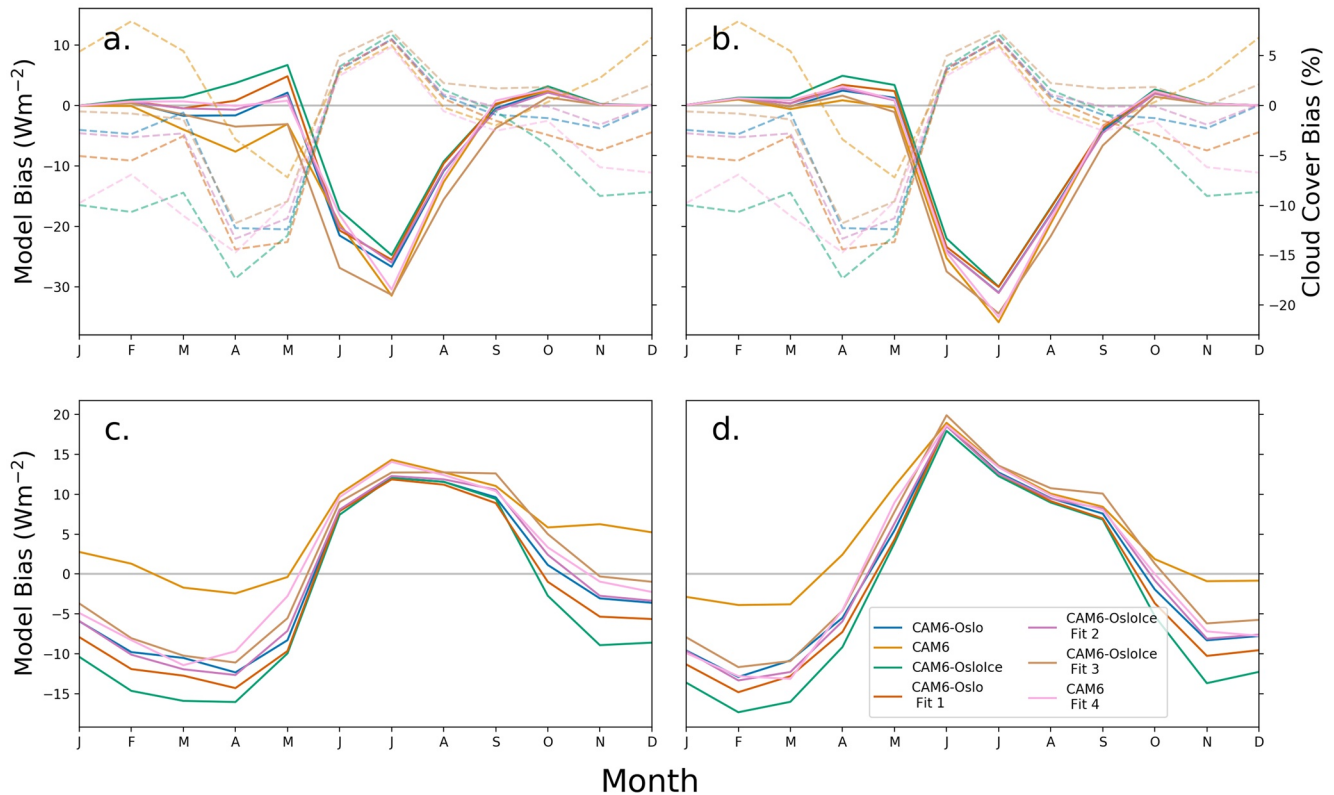

Figure 3. Monthly values for: (a) Model bias in shortwave downwelling flux at the surface (solid) and total cloud fraction (dashed), (b) Model bias in surface shortwave cloud radiative effect (solid) and total cloud fraction (dashed), (c) Model bias in longwave downwelling flux at the surface, (d) Model bias in surface longwave cloud radiative effect.
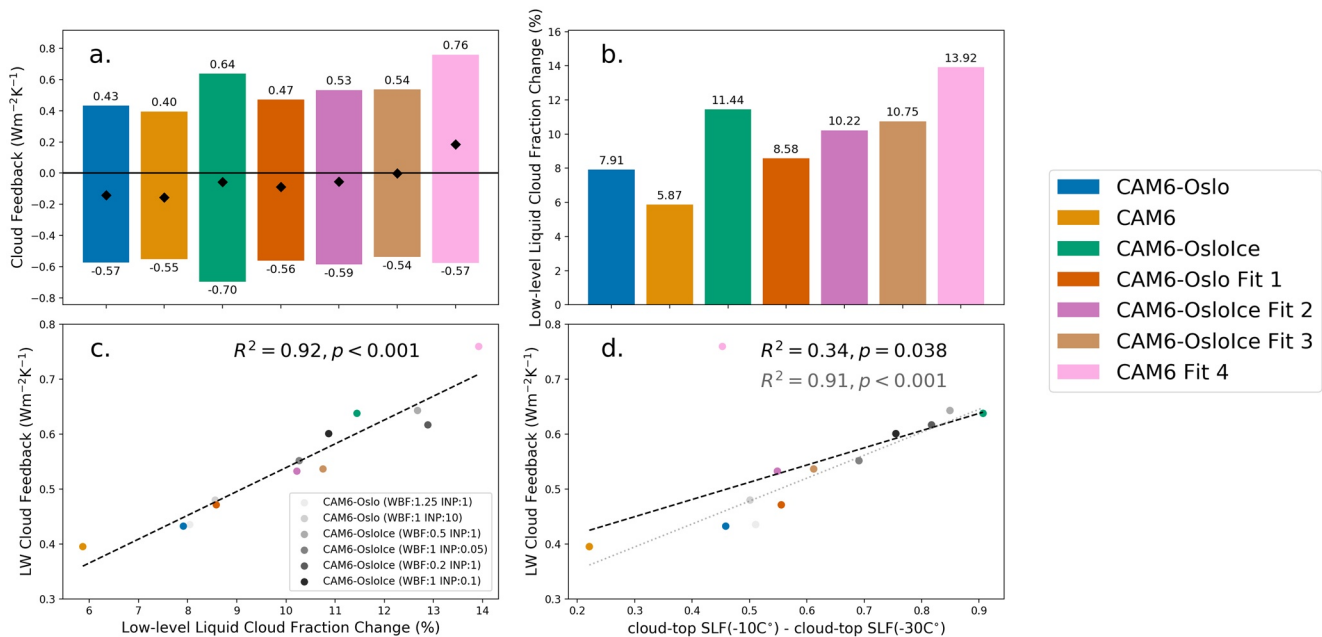
Figure 4. (a) Arctic-averaged longwave and shortwave cloud feedback. Diamonds denote the net cloud feedback. Kernel calculations do not incorporate surface albedo changes with mean state when calculating shortwave cloud feedback and tend to overestimate the shortwave cooling effect of clouds at high latitudes. (b) Arctic-averaged change in low-level liquid cloud fraction between present-day and +4K simulations. (c) Longwave cloud feedback as a function of the mean change in low-level liquid cloud fraction from November to April. (d) Longwave cloud feedback as a function of the difference in cloud top SLF between the −10°C and −30°C isotherms. In panel (d), gray text and best fit lines represent analysis excluding CAM6 Fit 4.

make up roughly two thirds of the total cloud fraction during the summer months in our simulations (Figure S3 in Supporting Information S1). Because the shortwave CRE is similar between model runs, changes in mixed-phase microphysics impact the Arctic mainly through the longwave CRE in the winter and spring.

Like the shortwave, the downwelling longwave surface flux and CRE biases (Figures 3c and 3d) are also highly similar. There is strong seasonal variation in the longwave biases, with excess downward flux from clouds in the summer and insufficient downward flux in the winter. The positive summer biases occur when all models produce excess cloud fraction, but the negative wintertime biases occur even in the models that capture both cloud fraction and phase well. CAM6 is the only model to capture the downward flux despite overproducing winter cloud fraction, suggesting biases in cloud height and emission temperature across all simulations. While passive sensors and their corresponding satellite simulators are poorly suited to constrain this behavior, cloud height and opacity variables recently incorporated into the COSP2 Lidar simulator will allow this wintertime bias to be investigated in future versions of CAM (Guzman et al., 2017; A. L. Morrison et al., 2019).

3.3. Cloud Radiative Feedbacks

Computing cloud radiative feedbacks allows us to assess the relative importance of the long- and shortwave cloud feedback processes and to investigate their dependence on the present-day cloud state and cloud microphysical properties. Figure 4a shows the long- and shortwave cloud feedback parameters and the net cloud feedback for each model simulation.

Differences in present day cloud fraction and phase are greatest in the winter and spring, suggesting that mixed-phase processes impact cloud feedbacks most during this time. We investigate how low-level (cloud top pressure >680 mb) liquid cloud fraction changes between the present day and +4K warming simulations (Figure 4b) correlate with the longwave cloud feedback parameter, finding that the average change in low-level liquid cloud fraction from November through April is strongly correlated with the longwave feedback ($R^2 = 0.92$; Figure 4c). Individual correlations by month indicate that this pattern is consistent from November through April, whereas no correlation is found from May through October (Figure S4 in Supporting Information S1).

To investigate why different parametrizations give rise to these feedbacks, we propose that the slope of the SLF curves in Figure 1 should determine how quickly liquid clouds replace ice clouds during warming. Since the SLF metrics change little in our +4K simulations (Figure S5 in Supporting Information S1), cloud phase changes occur because atmospheric warming shifts clouds to warmer isotherms where liquid replaces ice. The SLF metrics effectively describe the sensitivity of cloud phase to warming, potentially offering a predictor of longwave cloud feedback. We approximate this sensitivity as the change in SLF between the −10C and −30C isotherms and correlate this value with the LW cloud feedback (Figure 4d). All but one model (CAM6 Fit 4) show agreement with the predicted relationship. We hypothesize that large ice crystal sizes in CAM6 Fit 4 (Table 1) depress ice cloud lifetimes and lead to a much larger increase in low-level liquid cloud amount under warming, but leave this question open for future work. Excluding CAM6 Fit 4 from our analysis (Figure 4d gray lines and text) demonstrates that the SLF metric can effectively predict the LW cloud feedback. These results demonstrate that different parametrizations of mixed-phase processes impact Arctic warming by modifying how low-level liquid clouds increase in response to warming.

4. Discussion and Conclusion

We find large differences in thermodynamic phase between cloud tops and interiors in satellite observations of Arctic mixed-phase clouds, consistent with previous ground-based measurements. CAM6-Oslo captures this vertical phase structure better than CAM6, suggesting that model aerosol schemes and high cloud parameterizations play an important role in determining cloud phase. We evaluate a significant model error that prevents heterogeneous and secondary nucleation processes from creating new ice crystals and find that cloud water is significantly reduced when these nucleation processes are able to operate freely.

All models produce insufficient cloud fraction in the spring and excess cloud fraction in the summer. The summer bias dominates the shortwave impact, leading to a net negative annual shortwave flux bias. Longwave flux biases are strongly seasonal, with positive summer biases explained by excess summer cloud fraction and negative winter biases likely resulting from low-biased cloud emission temperatures. The greatest variation between models occurs in the winter and spring, and changes in low-level liquid cloud fraction under warming during these seasons are strongly correlated with the longwave cloud feedback parameter. Our results indicate that the parametrization of mixed-phase microphysics influences the Arctic climate by modifying how winter and spring clouds respond to warming, and that cloud phase observations may constrain this relationship. Positive longwave cloud feedback associated with winter cloud fraction increases was also observed in fully coupled simulations of CESM1 (A. L. Morrison et al., 2019), raising to question the relative contributions of sea ice loss and simple surface warming to these winter feedbacks.

Our results demonstrate the need to capture local cloud phase processes in order to understand how mixed-phase cloud processes impact Arctic warming. Future studies should use multiple atmospheric components, and use fully-coupled models to determine whether the proposed constraint is valid in a dynamic climate system.

Data Availability Statement

CERES-EBAF L3 data are available online at the NASA Langley Atmospheric Sciences Data Center website (https://ceres.larc.nasa.gov/data/#ebaf-level-3). CALIOP L2 data used to derive SLF metrics can be freely downloaded (https://search.earthdata.nasa.gov/). The CALIOP GOCCP observational data set with cloud opacity variables from Guzman et al. (2017) can be downloaded from https://climserv.ipsl.polytechnique.fr/cfmip-obs/. ERA-Interim reanalysis data can be downloaded freely (https://www.ecmwf.int/en/forecasts/datasets/reanalysis-datasets/era-interim). Model data produced in this study are available at https://doi.org/10.5281/zenodo.5781706.

References

Boucher, O., Randall, D., Artaxo, P., Bretherton, C., Feingold, G., Forster, P., & Zhang, X. (2013). Clouds and aerosols [Book Section]. In Stocker, T. (Ed.), *Climate change 2013: The physical science basis. Contribution of working group I to the fifth assessment report of the intergovernmental panel on climate change* (pp. 571–658). Cambridge University Press. https://doi.org/10.1017/CBO9781107415324.016

Cesana, G., & Chepfer, H. (2012). How well do climate models simulate cloud vertical structure? A comparison between CALIPSO-GOCCP satellite observations and cmip5 models. *Geophysical Research Letters*, *39*(20). https://doi.org/10.1029/2012gl053153

Cesana, G., Kay, J. E., Chepfer, H., English, J. M., & de Boer, G. (2012). Ubiquitous low-level liquid-containing arctic clouds: New observations and climate model constraints from CALIPSO-GOCCP. *Geophysical Research Letters*, *39*(20). https://doi.org/10.1029/2012gl053385

Chepfer, H., Bony, S., Winker, D., Cesana, G., Dufresne, J. L., Minnis, P., & Zeng, S. (2010). The GCM-oriented CALIPSO cloud product (CA-LIPSO-GOCCP). *Journal of Geophysical Research*, *115*(D4). https://doi.org/10.1029/2009jd012251

Danabasoglu, G., Lamarque, J.-F., Bacmeister, J., Bailey, D. A., DuVivier, A. K., Edwards, J., & Strand, W. G. (2020). The community earth system model version 2 (CESM2). *Journal of Advances in Modeling Earth Systems*, *12*(2), e2019MS001916. https://doi.org/10.1029/2019ms001916

Dee, D. P., Uppala, S. M., Simmons, A. J., Berrisford, P., Poli, P., Kobayashi, S., & Vitart, F. (2011). The era-interim reanalysis: Configuration and performance of the data assimilation system. *Quarterly Journal of the Royal Meteorological Society*, *137*(656), 553–597. https://doi.org/10.1002/qj.828

Eyring, V., Bony, S., Meehl, G. A., Senior, C. A., Stevens, B., Stouffer, R. J., & Taylor, K. E. (2016). Overview of the Coupled Model Intercomparison Project Phase 6 (CMIP6) experimental design and organization. *Geoscientific Model Development*, *9*(5), 1937–1958. https://doi.org/10.5194/gmd-9-1937-2016

Feldl, N., Po-Chedley, S., Singh, H. K. A., Hay, S., & Kushner, P. J. (2020). Sea ice and atmospheric circulation shape the high-latitude lapse rate feedback. *NPJ Climate and Atmospheric Science*, *3*(1), 41. https://doi.org/10.1038/s41612-020-00146-7

Fridlind, A. M., Ackerman, A. S., McFarquhar, G., Zhang, G., Poellot, M. R., DeMott, P. J., & Heymsfield, A. J. (2007). Ice properties of single-layer stratocumulus during the mixed-phase arctic cloud experiment: 2. Model results. *Journal of Geophysical Research*, *112*(D24). https://doi.org/10.1029/2007jd008646

Fu, S., Deng, X., Shupe, M. D., & Xue, H. (2019). A modelling study of the continuous ice formation in an autumnal arctic mixed-phase cloud case. *Atmospheric Research*, *228*, 77–85. https://doi.org/10.1016/j.atmosres.2019.05.021

Gettelman, A. (2021). *Issue #20 escomp/pumas*. Retrieved from https://github.com/ESCOMP/PUMAS/issues/20

Goosse, H., Kay, J. E., Armour, K. C., Bodas-Salcedo, A., Chepfer, H., Docquier, D., & Vancoppenolle, M. (2018). Quantifying climate feedbacks in polar regions. *Nature Communications*, *9*(1), 1919. https://doi.org/10.1038/s41467-018-04173-0

Guzman, R., Chepfer, H., Noel, V., Vaillant de Guélis, T., Kay, J. E., Raberanto, P., & Winker, D. M. (2017). Direct atmosphere opacity observations from CALIPSO provide new constraints on cloud-radiation interactions. *Journal of Geophysical Research: Atmospheres*, *122*(2), 1066–1085. https://doi.org/10.1002/2016jd025946

Hobbs, P. V., & Rangno, A. L. (1998). Microstructures of low and middle-level clouds over the Beaufort Sea. *Quarterly Journal of the Royal Meteorological Society*, *124*(550), 2035–2071. https://doi.org/10.1002/qj.49712455012

Hoose, C., Lohmann, U., Bennartz, R., Croft, B., & Lesins, G. (2008). Global simulations of aerosol processing in clouds. *Atmospheric Chemistry and Physics*, *8*(23), 6939–6963. https://doi.org/10.5194/acp-8-6939-2008

Huang, Y., Dong, X., Kay, J. E., Xi, B., & McIlhattan, E. A. (2021). The climate response to increased cloud liquid water over the arctic in CESM1: A sensitivity study of Wegener–Bergeron–Findeisen process. *Climate Dynamics*, *56*(9), 3373–3394. https://doi.org/10.1007/s00382-021-05648-5

Jiang, H., Cotton, W. R., Pinto, J. O., Curry, J. A., & Weissbluth, M. J. (2000). Cloud resolving simulations of mixed-phase arctic stratus observed during base: Sensitivity to concentration of ice crystals and large-scale heat and moisture advection. .*Journal of the Atmospheric Sciences*, *57*(13), 210522–212117. https://doi.org/10.1175/1520-0469(2000)057<2105:crsomp>2.0.co;2

Kato, S., Rose, F. G., Rutan, D. A., Thorsen, T. J., Loeb, N. G., Doelling, D. R., & Ham, S.-H. (2018). Surface irradiances of edition 4.0 clouds and the earth's radiant energy system (CERES) energy balanced and filled (EBAF) data product. *Journal of Climate*, *31*(11), 4501–4527. https://doi.org/10.1175/jcli-d-17-0523.1

Kay, J. E., L'Ecuyer, T., Chepfer, H., Loeb, N., Morrison, A., & Cesana, G. (2016). Recent advances in arctic cloud and climate research. *Current Climate Change Reports*, *2*(4), 159–169. https://doi.org/10.1007/s40641-016-0051-9

Kirkevåg, A., Grini, A., Olivié, D., Seland, Ø., Alterskjær, K., Hummel, M., & Iversen, T. (2018). A production-tagged aerosol module for earth system models, osloaero5.3 – Extensions and updates for cam5.3-oslo. *Geoscientific Model Development*, *11*(10), 3945–3982. https://doi.org/10.5194/gmd-11-3945-2018

Komurcu, M., Storelvmo, T., Tan, I., Lohmann, U., Yun, Y., Penner, J. E., & Takemura, T. (2014). Intercomparison of the cloud water phase among global climate models. *Journal of Geophysical Research: Atmospheres*, *119*(6), 3372–3400. https://doi.org/10.1002/2013jd021119

Korolev, A. (2007). Limitations of the Wegener–Bergeron–Findeisen mechanism in the evolution of mixed-phase clouds. *Journal of the Atmospheric Sciences*, *64*(9), 3372–3375. https://doi.org/10.1175/JAS4035.1

Lenaerts, J. T. M., Gettelman, A., Van Tricht, K., van Kampenhout, L., & Miller, N. B. (2020). Impact of cloud physics on the Greenland ice sheet near-surface climate: A study with the community atmosphere model. *Journal of Geophysical Research: Atmospheres*, *125*(7), e2019JD031470. https://doi.org/10.1029/2019jd031470

Lenaerts, J. T. M., Van Tricht, K., Lhermitte, S., & L'Ecuyer, T. S. (2017). Polar clouds and radiation in satellite observations, reanalyses, and climate models. *Geophysical Research Letters*, *44*(7), 3355–3364. https://doi.org/10.1002/2016gl072242

Liu, X., Ma, P.-L., Wang, H., Tilmes, S., Singh, B., Easter, R. C., & Rasch, P. J. (2016). Description and evaluation of a new four-mode version of the modal aerosol module (mam4) within version 5.3 of the community atmosphere model. *Geoscientific Model Development*, *9*(2), 505–522. https://doi.org/10.5194/gmd-9-505-2016

Matus, A. V., & L'Ecuyer, T. S. (2017). The role of cloud phase in earth's radiation budget. *Journal of Geophysical Research: Atmospheres*, *122*(5), 2559–2578. https://doi.org/10.1002/2016jd025951

Mauritsen, T., Stevens, B., Roeckner, E., Crueger, T., Esch, M., Giorgetta, M., & Tomassini, L. (2012). Tuning the climate of a global model. *Journal of Advances in Modeling Earth Systems*, *4*(3). https://doi.org/10.1029/2012ms000154

McIlhattan, E. A., L'Ecuyer, T. S., & Miller, N. B. (2017). Observational evidence linking arctic supercooled liquid cloud biases in CESM to snowfall processes. *Journal of Climate*, *30*(12), 4477–4495. https://doi.org/10.1175/JCLI-D-16-0666.1

Mitchell, J. F. B., Senior, C. A., & Ingram, W. J. (1989). CO_2 and climate: A missing feedback? *Nature*, *341*(6238), 132–134. https://doi.org/10.1038/341132a0

Morrison, A. L., Kay, J. E., Chepfer, H., Guzman, R., & Yettella, V. (2018). Isolating the liquid cloud response to recent arctic sea ice variability using spaceborne lidar observations. *Journal of Geophysical Research: Atmospheres*, *123*(1), 473–490. https://doi.org/10.1002/2017jd027248

Morrison, A. L., Kay, J. E., Frey, W. R., Chepfer, H., & Guzman, R. (2019). Cloud response to arctic sea ice loss and implications for future feedback in the CESM1 climate model. *Journal of Geophysical Research: Atmospheres*, *124*(2), 1003–1020. https://doi.org/10.1029/2018jd029142

Morrison, H., de Boer, G., Feingold, G., Harrington, J., Shupe, M. D., & Sulia, K. (2012). Resilience of persistent arctic mixed-phase clouds. *Nature Geoscience*, *5*(1), 11–17. https://doi.org/10.1038/ngeo1332

Morrison, H., & Gettelman, A. (2008). A new two-moment bulk stratiform cloud microphysics scheme in the community atmosphere model, version 3 (CAM3). Part i: Description and numerical tests. *Journal of Climate*, *21*(15), 3642–3659. https://doi.org/10.1175/2008JCLI2105.1

Pithan, F., & Mauritsen, T. (2014). Arctic amplification dominated by temperature feedbacks in contemporary climate models. *Nature Geoscience*, *7*(3), 181–184. https://doi.org/10.1038/ngeo2071

Prenni, A. J., Demott, P. J., Rogers, D. C., Kreidenweis, S. M., Mcfarquhar, G. M., Zhang, G., & Poellot, M. R. (2009). Ice nuclei characteristics from m-pace and their relation to ice formation in clouds. *Tellus B: Chemical and Physical Meteorology*, *61*(2), 436–448. https://doi.org/10.1111/j.1600-0889.2009.00415.x

Seland, Ø., Bentsen, M., Seland Graff, L., Olivié, D., Toniazzo, T., Gjermundsen, A., & Schulz, M. (2020). The Norwegian earth system model, noresm2 – Evaluation of thecmip6 deck and historical simulations. *Geoscientific Model Development Discussions*, 1–68. https://doi.org/10.5194/gmd-2019-378

Shupe, M. D., & Intrieri, J. M. (2004). Cloud radiative forcing of the arctic surface: The influence of cloud properties, surface albedo, and solar zenith angle. *Journal of Climate*. *17*(3), 616–628. https://doi.org/10.1175/1520-0442(2004)017<0616:crfota>2.0.co;2

Soden, B. J., Held, I. M., Colman, R., Shell, K. M., Kiehl, J. T., & Shields, C. A. (2008). Quantifying climate feedbacks using radiative kernels. *Journal of Climate*, *21*(14), 3504–3520. https://doi.org/10.1175/2007jcli2110.1

Swales, D. J., Pincus, R., & Bodas-Salcedo, A. (2018). The cloud feedback model intercomparison project observational simulator package: Version 2. *Geoscientific Model Development*, *11*(1), 77–81. https://doi.org/10.5194/gmd-11-77-2018

Tan, I., & Storelvmo, T. (2016). Sensitivity study on the influence of cloud microphysical parameters on mixed-phase cloud thermodynamic phase partitioning in CAM5. *Journal of the Atmospheric Sciences*, *73*(2), 709–7281. https://doi.org/10.1175/jas-d-15-0152.1

Tan, I., & Storelvmo, T. (2019). Evidence of strong contributions from mixed-phase clouds to arctic climate change. *Geophysical Research Letters*, *46*(5), 2894–2902. https://doi.org/10.1029/2018gl081871

Taylor, K. E., Stouffer, R. J., & Meehl, G. A. (2012). An overview of cmip5 and the experiment design. *Bulletin of the American Meteorological Society*, *93*(4), 485–4981. https://doi.org/10.1175/bams-d-11-00094.1

Winker, D. M., Vaughan, M. A., Omar, A., Hu, Y., Powell, K. A., Liu, Z., & Young, S. A. (2009). Overview of the CALIPSO mission and CALIOP data processing algorithms. *Journal of Atmospheric and Oceanic Technology*, *26*(11), 2310–2323. https://doi.org/10.1175/2009JTECHA1281.1

Zelinka, M. D., Myers, T. A., McCoy, D. T., Po-Chedley, S., Caldwell, P. M., Ceppi, P., & Taylor, K. E. (2020). Causes of higher climate sensitivity in cmip6 models. *Geophysical Research Letters*, *47*(1), e2019GL085782. https://doi.org/10.1029/2019gl085782

Zhu, J., Otto-Bliesner, B. L., Brady, E. C., Poulsen, C., Shaw, J. K., & Kay, J. E. (2021). LGM paleoclimate constraints inform cloud parameterizations and equilibrium climate sensitivity in CESM2. *Earth and Space Science Open Archive*, *49*. https://doi.org/10.1002/essoar.10507790.1

References From the Supporting Information

Bruno, O., Hoose, C., Storelvmo, T., Coopman, Q., & Stengel, M. (2021). Exploring the cloud top phase partitioning in different cloud types using active and passive satellite sensors. *Geophysical Research Letters*, *48*(2), e2020GL089863. https://doi.org/10.1029/2020gl089863

DeMott, P. J., Prenni, A. J., Liu, X., Kreidenweis, S. M., Petters, M. D., Twohy, C. H., & Rogers, D. C. (2010). Predicting global atmospheric ice nuclei distributions and their impacts on climate. *Proceedings of the National Academy of Sciences*, *107*(25), 11217–11222. https://doi.org/10.1073/pnas.0910818107

Tan, I., Storelvmo, T., & Zelinka, M. D. (2016). Observational constraints on mixed-phase clouds imply higher climate sensitivity. *Science*, *352*(6282), 224–227. https://doi.org/10.1126/science.aad5300